Check for
updates

Statistical analysis of shoreline change reveals erosion and baseline are increasing off the northern Tamil Nadu Coasts of India

German Amali Jacintha Thomas[ID] ·
Radhika Rajasree Santha Ravindranath[ID] · Sriganesh Jeyagopal[ID] ·
Suman Thodhal Yoganandham[ID]

Abstract Many tourists have been recently attracted towards the coasts around the world, especially to the large urban centres and economically significant areas. In the last four decades, there is a significant increase in the key coastal developments and tourist's attractions like major ports, minor ports, fishing harbours, desalination plants, shore protection structures, and many more along the southeast coasts of India, in particular, northern Tami Nadu coastal stretches. The shoreline change study of these regions were carried out using the geospatial technologies (satellite remote sensing and geographical information system) to examine potential modifications occurred during the last 32 years between March 1990 and May 2022. This study used Landsat satellite images of spatial resolution 30 m to track the shoreline changes which was extracted using the Digital Image Processing software and techniques. In addition, the United States Geological Survey (USGS) developed Digital Shoreline Analysis System (DSAS) v5.2 software, an add-on tool to ArcGIS used for the statistical analysis to compute the shoreline rate of change. The linear regression rate (LRR) and end point rate (EPR) statistics were used to identify the eroding, accreting, and stable shoreline between Kattupalli coast and Kalpakkam coast of the northern Tamil Nadu coasts. This shoreline study of 106 km was carried out by dividing it into six zones (zone 1 to zone 6), and the DSAS analysis conveys that the shoreline of zone 1 (Kattupalli) and zone 2 (Ennore) shows erosion compared to other four zones. In locations where the coast is vulnerable, national mitigation measures must be implemented.

Keywords Satellite image · Erosion · Accretion · Rate of change

G. Thomas
Centre for Remote Sensing and Geo-informatics,
Sathyabama Institute of Science and Technology, Chennai,
Tamil Nadu, India

G. Thomas · R. Santha Ravindranath ·
S. Thodhal Yoganandham (✉)
Centre for Ocean Research, Sathyabama Institute
of Science and Technology, Chennai, Tamil Nadu, India
e-mail: sumancas2010@gmail.com

R. Santha Ravindranath
Faculty of Fisheries, Kerala University of Fisheries
and Ocean Studies, Cochin, Kerala, India

S. Jeyagopal
National Technology Centre for Ports, Waterways
and Coasts, Indian Institute of Technology Madras,
Chennai, Tamil Nadu, India

S. Thodhal Yoganandham
Department of Environmental Engineering, Changwon
National University, Changwon, Gyeongsangnamdo,
Republic of Korea

Introduction

The extraction of shorelines should be seen as a crucial area for study from the standpoint of coastal zone monitoring, which is important for national development and environmental management (Rasuly et al., 2010). The International Geographic Data Committee (IGDC) acknowledges that the coastline is one of the most prominent distinguishing characteristics. The boundary between a land and a body of water is known as its coastline (Li et al., 2001). A coastal location, orientation, and geometric shape data are crucial for geographical exploration, autonomous navigation, coastal erosion modelling and monitoring, and coastal resource management and inventory (Liu & Jezek, 2004). One of the most active processes in coastal areas is shoreline change (Bagli & Soille, 2003; Mills et al., 2005). Dense populations near the beach generate more susceptible places in many coastal zones of emerging nations. Therefore, mapping the shoreline shift is crucial for coastal hazard assessment (Marfai et al., 2008).

The coastline is a highly dynamic structure that indicates coastal erosion and accretion, as Genz et al. (2007) described. Various time ranges, geological to transient severe occurrences, are involved in shoreline modifications. Waves, tides, winds, sea level rise, frequent storms, geomorphic processes such as accretion and erosion, and human activities are all significant contributors to these alterations (Van & Binh, 2009). Therefore, coastal resource management, coastal environment conservation, sustainable coastal development, and planning all rely heavily on accurate and up-to-date shoreline maps and monitoring (Li & Tang, 2013; Roy et al., 2018; Sherman & Bauer, 1993). Thus, it is crucial to extract shorelines at different periods and precisely estimate future coastal changes, focusing on rapid and accurate assessments of dynamic shoreline changes (Berberoglu & Akin, 2009; Chen et al., 2019).

Remote sensing is more effective for coastal and deltaic environment monitoring than traditional approaches (Saranathan et al., 2011). Over the last several years, there has been a lot of focus on using numerical modelling and remote sensing data to assess and predict shoreline change (Raj et al., 2020). Primary change estimations are made more precisely and accurately using remotely sensed satellite data and GIS technologies (Kaliraj et al., 2015). Monitoring coastal changes is made possible through the study of multi-temporal Landsat satellite image (MTLSI) series utilizing sensors including the Thematic Mapper (TM), Multi-Spectral Scanner (MSS), and Enhanced Thematic Mapper Plus (ETM+), as well as classifications based on Tasseled cap, ISO data clustering, maximum likelihood, normalized difference vegetation index (NDVI), and principal component analysis (PCA) (Mujabar & Chandrasekar, 2013). Shoreline change rates have been estimated using a variety of statistical techniques, including least median of squares (LMS), LRR, EPR, average rate (AOR), and Jack Knifing (Deepika et al., 2014). However, EPR was viewed by Dolan et al. (1991) as the best method for assessing the long-term changes to the coastline. When determining the location of the coastline, the LRR also plays a crucial role by minimizing the effects of random error and temporary variations (Maiti & Bhattacharya, 2009). The EPR, LRR, and LMS modules of the Digital Shoreline Analysis System (DSAS) are statistical methods that help to quantify shoreline change over time using satellite images (Thieler et al., 2017). MSS satellite data, including Landsat TM, ETM, OLI pictures, and DSAS, have been utilized effectively by Nassar et al. (2018) to identify shoreline alterations along the coast of northern Sinai (Egypt).

Multiple scientists, including Natesan et al. (2015), Kumaravel et al. (2013), and Chand and Acharya (2010) have tracked coastal shifts in Tamil Nadu. In addition, Kannan et al. (2014) have reported on the wave energy along the research region, while Anand et al. (2011) goes into depth about the direction and amount of littoral drift through measurements. However, according to the literature review on a littoral ridge along the Chennai coast, there is a severe deficiency in accurately measuring the shoreline change rates using high-precision methodologies. This research is the first to examine the coastline alterations over a 106-km stretch of three coastal districts in Tamil Nadu: Thiruvallur, Chennai, and Chengalpattu. These districts include both urban and semi-urban regions of the city of Chennai. Herein, the results of a 32-year-long Digital Shoreline Analysis System (DSAS) calculation projecting how the coastline has changed are detailed. This research intends to map and quantify coastal erosion and accretion rates throughout the study region using many statistical methodologies made possible by DSAS, such as the EPR and the LRR.

Materials and methods

Study area

The Indian state of Tamil Nadu is the eastern coast and southernmost state in the country. Northern Tamil Nadu coastline comprises Thiruvallur, Chennai, and Chengalpattu districts (Fig. 1). Tamil Nadu has the sixth-highest population in India according to Census 2011 (at 72,147,030), with over half of its residents residing around its coasts. A total of 1,664,105 people live in the region, with Thiruvallur district accounting for around 3,728,104 of those people, Chennai district for roughly 8,917,749, and Chengalpattu district for approximately 3,998,252 people. The study region is the most populated part of the state and its economic
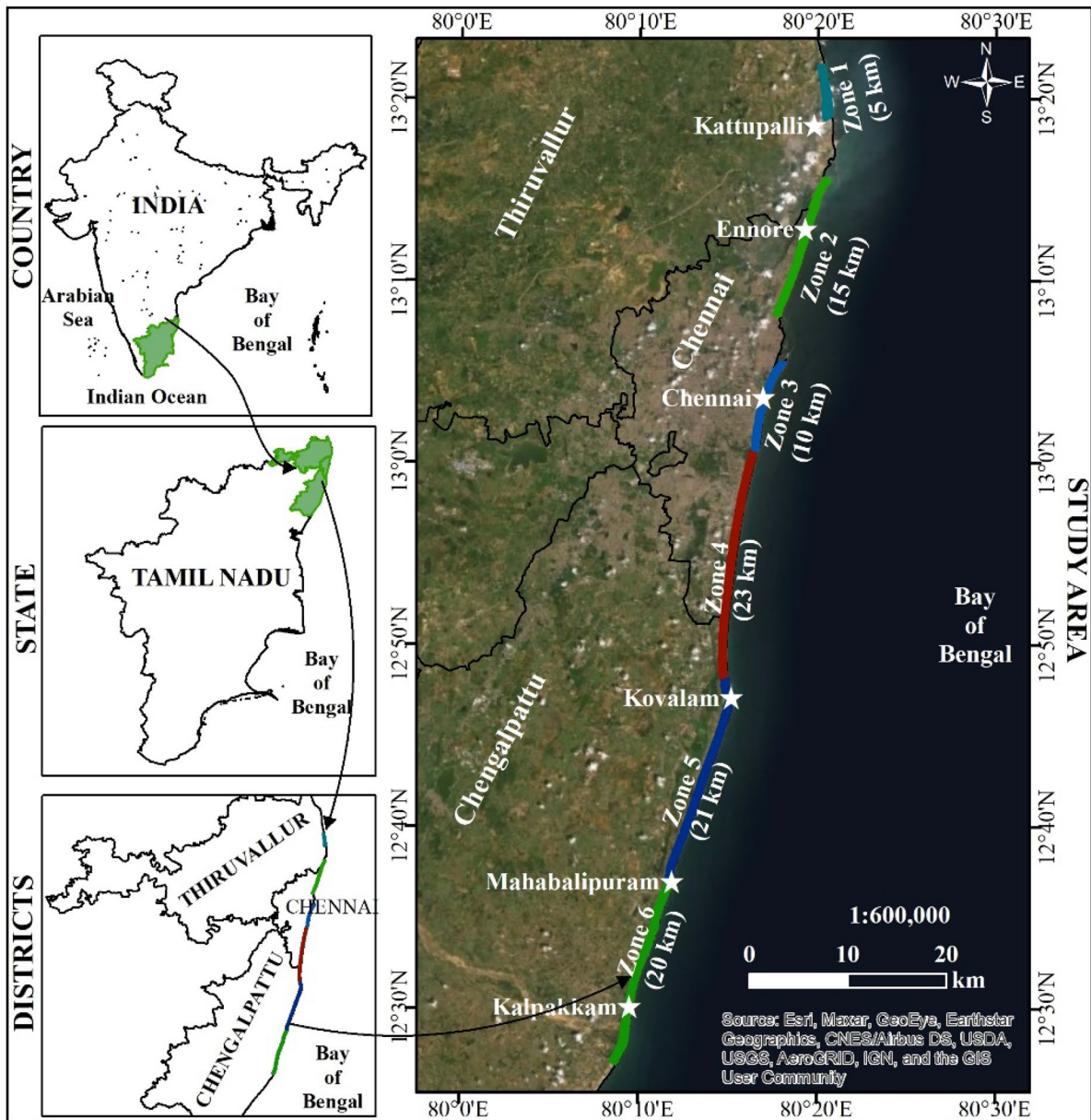
Fig. 1 Study area map of northern Tamil Nadu, India

hub. The geographical coordinates of this coastline study area are between the latitude 13° 22′ 2″N and 12° 26′ 53″N and also between the longitude 80° 20′ 16″E and 80° 8′ 39″E. There are a total of 106 km of coastline within the study region; this includes 29 km of the Thiruvallur district coastline, 19 km of the Chennai district coastline, and 58 km of the Chengalpattu district coastline. Each year, short-term natural and man-made disruptions impact the northern Tamil Nadu coast (Saranathan et al., 2011). Ports of Kattupalli (zone 1), Ennore (zone 2), and Chennai (zone 3) and groins in Ennore are examples of man-made structures in northern Tamil Nadu coastal zone, zone 4 includes the world's second-longest beach, Marina Beach; zone 5 includes Mamallapuram Beach, and zone 6 includes the Kalpakkam Atomic Power Energy Station which are all at high risk (Pandian et al., 2004). Semi-diurnal tides with average micro-tidal neap and spring tidal ranges between 0.1 and 1.4 m are observed throughout the northern Tamil Nadu coast (Kankara et al., 2013).

Shoreline extraction

MTLSI between 1990 and 2022 were used in this study. The satellite images were downloaded from the USGS website for the years 1990, 1995, 2000, 2005, 2010, 2015, 2020, and 2022. Landsat data were sampled at every 5-year interval to capture the medium-term variation of the shoreline between 1990 and 2022 (Table 1). Only one image acquisition data was selected from the specified years, and this was based on the main cloudless imagery, as cloud may affect the shoreline position detection, and hence image acquired in summer months between March and June. Each satellite image was downloaded in UTM (Universal Transverse Mercator) projection with WGS 84 datum and Zone 44 North. To study shoreline changes, the satellite images are to be geometrically corrected. The georeferenced satellite images were co-registered using imagine auto-sync workstation to make the geometric correction accurately. The corresponding image tie points between the reference, and input images were identified and measured using the Automated Point Measurement (APM) software tool, which uses image-matching technology. In general, two or more images that are already georeferenced were co-registered with the reference image that is 2022 satellite image. The tie points were generated using an automatic tie point

Table 1 Landsat satellite image details used for this shoreline change

S.no	Satellite and sensor	Spatial resolution	Date of acquisition
1	Landsat TM 5	30 m	15.3.1990
2	Landsat TM 5	30 m	29.3.1995
3	Landsat ETM 5	30 m	5.5.2000
4	Landsat TM 5	30 m	11.5.2005
5	Landsat TM 5	30 m	25.5.2010
6	Landsat 8	30 m	24.6.2015
7	Landsat 8	30 m	2.4.2020
8	Landsat 8	30 m	26.5.2022

measurement tool for both the reference image and the input image. So, all the images were matched with tie points generated with the reference image. The accuracy of the image is based on the reference image. Root Mean Square Error (RMSE) values were considered while doing co-registration. The output image was stored using the appropriate resampling method. This process was done for all images keeping the same reference images. The shorelines for each year were digitized and saved along with the appropriate MM/DD/YYYY added to the attribute table.

Shoreline analysis in DSAS

To calculate changes, we used the USGS Digital Shoreline Analysis System (DSAS) version 5.2 (a plug-in for ArcGIS). DSAS is a software extension used in measuring, quantifying, calculating, and monitoring shoreline rate-of-change statistics from multiple historical shoreline positions and sources. The procedures consisted of four stages: preparing the shoreline, establishing a baseline, generating transects, and calculating the rate of change (Raj et al., 2020). First, a single shape file with all shorelines was uploaded to a personal geodatabase. Then, shoreline layer properties were modified to include the date in the format MM/DD/YYYY, and the baseline was given in metres relative to a projected coordinate system. Next, a landward baseline was created by a 1000-m buffer from the most recent and landward shoreline (2022). Finally, the buffer polygon was converted into polylines. This baseline is the starting point for all transects cast. This was added to the Geodatabase as a feature class. Next, the default parameters were set for casting transects.

Using the cast transects feature in DSAS, placed transects for 1000 m perpendicular to the shore at 100-m intervals over the whole shoreline, smoothing over a distance of 50 m. Data from the transect feature were utilized to calculate the shifts, and 1054 transects were generated for this purpose. This investigation employed the LRR and EPR as statistical tools. Positive values were found for accretion and negative values for erosion when comparing the rates of shoreline fluctuation (Raj et al., 2020; Natesan et al., 2015). After the data analysis, a table containing the results was generated and stored in the same user-controlled Geodatabase.

Statistical analysis

The variation rate may be estimated using LRR by fitting a least-square regression line to each transect point's location along the shoreline (DSAS 5.0 user guide 2018). This approach incorporates all available data without regard to variations in trend or precision. The whole computational calculation was based on the well-established statistical ideas of Crowell et al. (1997) and Dolan et al. (1991). It is the best way to anticipate where the water's edge will be and how much uncertainty there will be in that prediction (Douglas & Crowell, 2000; Crowell et al., 1997). Another statistical metric, known as net shoreline movement (NSM), calculates the difference between transects that are parallel to the shorelines and the separation between the recent and oldest shorelines (DSAS 5.0 user guide 2018). Its numerical expression is:

$$NSM = \{d_{2022} - d_{1990}\}m$$

To get the EPR, NSM was split according to the interval between the oldest and most recent shoreline (Himmelstoss et al., 2021). Therefore, it requires at least two shoreline dates as well as, preferably, additional information on accretion and erosion (Crowell et al., 1997; Dolan et al., 1991). The following is the formula used to determine EPR:

$$EPR = \{\frac{d_{2022} - d_{1990}}{t_{2022} - t_{1990}}\}m/year$$

where d is the distance between the shoreline and baselines, t the dates of the two shoreline positions, and $m/year$ rate of changes.

All data analysis was done using GraphPad Prism1 8.0 (Graphpad Inc., Harvey Motulsky, Los Angeles, CA, USA). At first, a descriptive analysis was performed to provide an overall view of LRR, EPR, and shoreline position from the baseline of zone 1, zone 2, zone 3, zone 4, zone 5, and zone 6 over the study period. Then, an LRR was used to fit the shorelines offset from the starting position to each independent variable. Statistical significance was defined as a p-value less than < 0.05.

Result and discussion

DSAS attempted to predict the coastline changes using satellite images of the last 32 years between 1990 and 2022. After post-processing the 32 years of satellite images in digital image processing software, shoreline analysis was carried out along the northern Tamil Nadu coasts about 104 km between the Kattupalli creek at Thiruvallur district on the north and the Kadalur village (latitude 12°26′53″N and longitude 80° 8′39″E) at Chengalpattu district on the south. The salient natural and anthropogenic geomorphic features within this region are four major natural rivers (Kosasthalaiyar, Coovum, Adyar, and Palar) joining into the Bay of Bengal, Kamarajar Port Limited (KPL) and Chennai Port Authority (ChPA), one minor port (Kattupalli Port), two fishing harbours (Kasimedu Fishing Harbour and New Thiruvotriyur Fishing Harbour), Madras Atomic Power Station (MAPS, Kalpakkam), archaeological sites (Mahabalipuram shore temple and Tiger Caves), two desalination plants (Kattupalli and Nemmeli), world second longest sandy beach (Marina Beach), tourist beaches (Elliot's Beach, Thiruvanmiyur Beach, Kovalam Rock Beach, etc.), two creeks (Ennore and Kattupalli), seawall, breakwater, groins, backwaters (Muttukadu and Kalpakkam), government and private beach resorts, fishing hamlets, etc. In some regions mentioned above, with evidence of major morphological changes between 1990 and 2022, few parts show relatively low or no changes, and few areas are stable coasts (Fig. 2a). The DSAS tool was used to produce 1054 transects, out of which 951 transects were used for the computation of the rate of shoreline change, and each zone's total used transects are zone 1, 58 transects (Table S2); zone 2, 152 transects (Table S5);

zone 3, 96 transects (Table S8); zone 4, 236 transects (Table S11); zone 5, 215 transects (Table S14); and zone 6, 194 transects (Table S17) to assess the coastline change in the study region. Each shoreline is about 100 m apart and runs 1000 m perpendicular from the baseline of the respective year shorelines for the linear measurements. Once the data from each profile is collected, EPR and LRR are used to determine the average annual rate of shoreline change (m/y). The highest accretion rates of 23.24 m/year (EPR) and 24.46 m/year (LRR) and maximum erosion rates of − 11.15 m/year (EPR) and − 12.24m/year (LRR) were recorded in the northern Tamil Nadu coastline (Fig. 2b) (Table 2). At each transect, we calculated the positional uncertainty between adjacent segments and the rate at which the coastline changed. Different techniques, such as LRR and EPR, were used to evaluate shoreline change rates. After comparing LRR with EPR, the R^2 value was found to be 0.97, with a significant level of statistical significance ($p < 0.0001$) (Fig. 2c) (Table S1). Therefore, it can be concluded that a significant difference in LRR vs EPR was discovered at a given transect when the rate of shoreline change was calculated. This study split the coastline of northern Tamil Nadu into six zones: (a) Kattupalli (zone 1), (b) Ennore (zone 2), (c) Chennai (zone 3), (d) Kovalam (zone 4), (e) Mahabalipuram (zone 5), and (f) Kalpakkam (zone 6).

Kattupalli (zone 1)

Ponneri and Thiruvotriyur taluks are located along the Thiruvallur district's shore. The combined coastline of these two taluks is 27.9 km in length. The estimated 53,007 people in the fishing community in 2012 were spread among 58 villages, 17 generating revenue, and a total of 28 fishing landing stations, as reported by the Tamil Nadu Department of Fisheries. The fishing industry has a strong presence in Pulicat, Minjur, Ennore, and Thiruvotriyur, whereas Kattupalli and other parts of the Thiruvallur district are among the most hazardous places. The shoreline length of about 6.00 km is discussed here between the northern breakwater of the M/s. Adani port earnest, M/s. Larson & Turbo port earnest, Kattupalli port, and north of the Kattupalli creek (latitude 13°21′45″N/longitude 80°20′15″E). Kattupalli creek is about 260–270 m in width and opens into the Bay of Bengal during the monsoon and typically closes during the non-monsoon/summer season. The 32 years of satellite images and the DSAS statistical analysis (EPR and LRR) convey that this region is typically dominated by erosion (Fig. 3a). The results indicate that the maximum shoreline accretion rate was about 0.19 m/y (EPR) and 0.01 m/y (LRR). It also found that the maximum erosion rate was − 11.15 m/y (EPR) and − 12.24 m/y (LRR). At Kattupalli, erosion was detected at an average rate of − 4.697 m/y (EPR) and − 5.259 m/y (LRR) (Fig. 3b, Table S2). Using WebGIS, Jayakumar and Malarvannan (2016) analysed shoreline changes in the same area from 1991 to 2006, and their findings are consistent with those of the present study. Due to man-made structures and groins, this researcher revealed that erosion along the Kattupalli shoreline reached a maximum of roughly 126 ha. Sriganesh et al. (2015) highlighted that the presence of coastal structures (breakwaters and groins) also influences this region's erosion. In 1990, the average baseline length was 845.7 m. The mean shoreline distance from baseline was 858.2 m in 1995, 866.5 m in 2000, 839.2 m in 2005, 828.5 m in 2010, 753.9 m in 2015, and 710.8 m in 2020 (Fig. 3c, Table S3). The coastline receded in 2022; as a result, it is now 694.5 m away from the baseline (Fig. 3c, Table S3). The coastline is reported to fluctuate throughout the year. A least-square regression line was fitted to all shoreline sites between 1990 and 2022 to get an LRR. In this study, regression coefficient (R^2) is 0.7982, $p < 0.05$ (Fig. 3d, Table S4). The results show a high correlation between the dependent and independent variables, as measured by R squared. Therefore, shoreline change was a significant correlation coefficient. The satellite images conclude that major shoreline changes were noticed between the northern breakwater of M/s. Adani port and 350 m north.

Ennore (zone 2)

Ennore coastal region is located in the north of the metropolitan city of Chennai, the capital of Tamil Nadu. This zone 2 region is bounded by the KPL on the north and Kasimedu fishing harbour (KFH) on the south, with a total 14.5 km length of coastline for the shoreline analysis. Ennore Port Limited (EPL) is one of the 12 major ports of the country and covers about 2.5 km of coastline by bordering two breakwaters (BW) on either side (one BW at the south and

Fig. 2 a Estimations of different shoreline changes (erosion or accretion) detected at northern coast in Tamil Nadu, India, between 1990 and 2022; **b** box plot of different degrees of erosion and accretion at the coast in Tamil Nadu, India, between 1990 and 2022 from LRR, EPR, **c** the correlation between shoreline rates obtained by different statistical methods (EPR, LRR) between 1990 and 2022. Blue dot represents data points, blue line represents line of regression, and red dashed lines represent the confidence interval
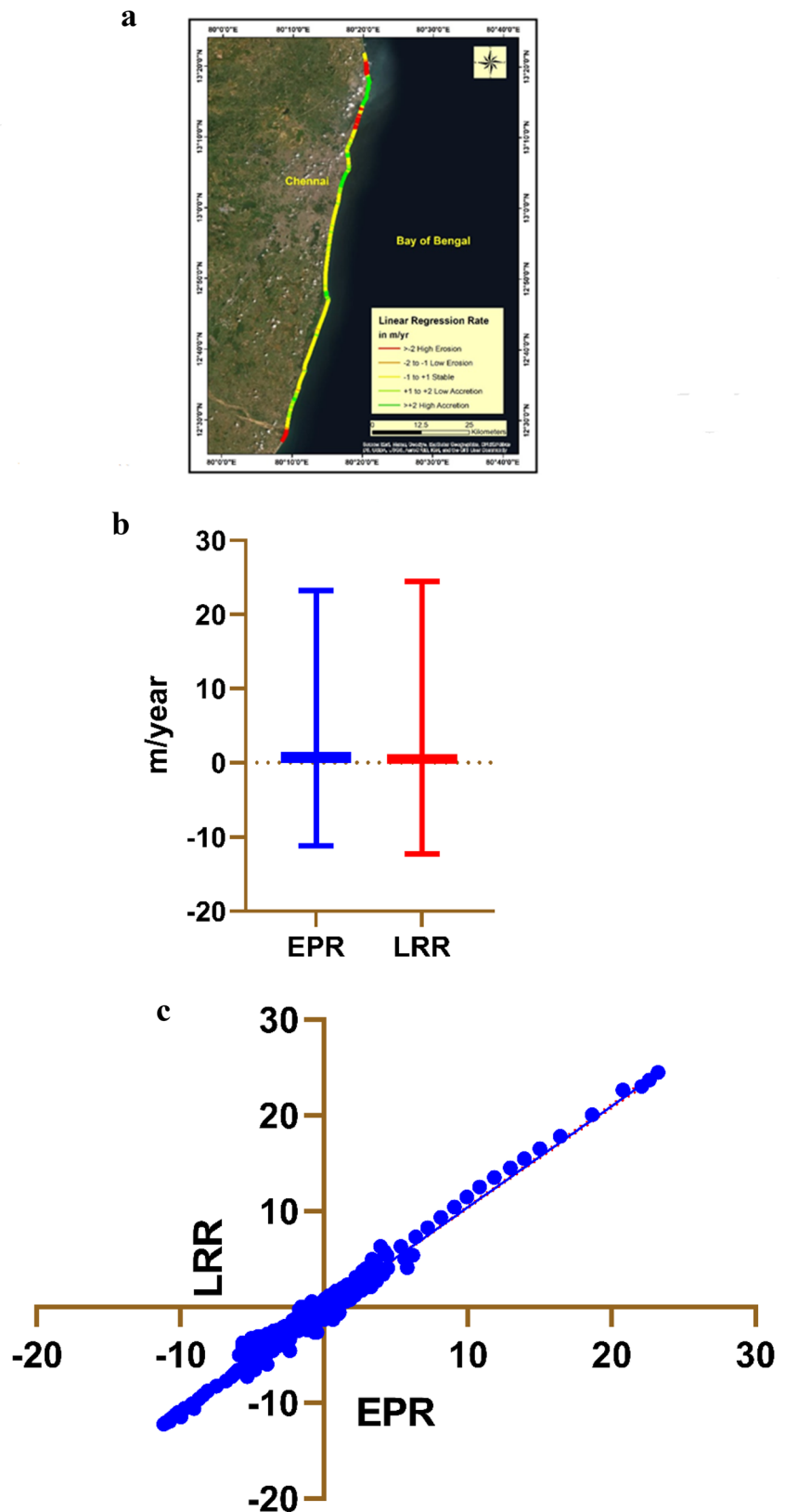
Table 2 Summary of EPR and LPR overall different shoreline changes detected at the northern coast in Tamil Nadu, India, between 1990 and 2022

	EPR	LRR
Number of values	1054	1054
Minimum	− 11.15	− 12.24
25% percentile	− 0.02000	− 0.1000
Median	0.7100	0.5150
75% percentile	1.483	1.173
Maximum	23.24	24.46
Range	34.39	36.70
Mean	1.019	0.8660
Std. deviation	3.955	4.135
Std. error of mean	0.1218	0.1274
Sum	1074	912.7

another BW at the north) of the port. KPL/EPL has a 630-m-wide opening towards the southeast direction (i.e. towards zone 2) for the boats/ships/vessels entry and exit, which is about 650 m offshore/perpendicular distance from the shoreline. Ennore Creek is situated at latitude 13°14′ N and longitude 80°19′40″ E, which is about 2.5 km south of the KPL south BW with a 450-m-wide opening into the Bay of Bengal. The satellite images between 2000 and 2022 show the Ennore creek (Kosasthalaiyar River mouth/joining into the Bay of Bengal) undergoes several modifications with erosion and accretions by closing/narrowing/widening of the opening along with the changes in the joining direction to the Bay of Bengal. The satellite images also show the coastal structures, like seawalls (parallel to the shore/coast) and groins (perpendicular to the shore/coast), in and around this river joins. The major shoreline change in Ennore coastal area is caused by the process of movements of sediments owing to the impact of physical factors. The coastline has been impacted by continuous natural sea waves, winds, currents, tides, the Kosasthalaiyar River, and anthropogenic activities (port, fishing, etc.). In 2001, the port was opened, so coal could be imported from nearby thermal power plants and used in future industrial developments. The coastal stretch of 14.5 km between the KPL/EPL and the Kasimedu Fishing Harbour (KFH) is shown in Fig. 4a with the coastal changes. Erosion was the dominant factor in this area. According to the findings, the maximum

coastline accretion rates were about 23.24 m/y (EPR) and 24.46 m/y (LRR). Maximum erosion rates were found to be − 5.41 m/y (EPR) and − 7.00 m/y (LRR) (Fig. 4b, Table S5). Raj et al. (2019) analysed coastal changes from 2013 to 2016 using LRR and EPR, and their findings are compared here. In the starting period of 1990, the mean baseline was 818.3 m. The mean baseline was 805.7 m in 1995, 541.5 m in 2000, 292.8 m in 2005, 191.2 m in 2010, 78.58 m in 2015, and 123.6 m in 2020. The coastline eroded throughout 2022, and the existing shoreline is 245.4 m from baseline (Fig. 4c, Table S6). The unstoppable spatial changes of the coastline/shores occur regularly at various scales. Its temporal changes can identify easily at/along the typical natural geomorphological features (sandy beach, rocky beach, estuary, inlet, creek, lagoon, backwater, river joining, tidal flats, etc.), also significantly at/along the anthropogenic interventions (seawall, groin, breakwater, pipeline, the fishing harbour, ports, etc.). We calculated an LRR of change by using a least-square regression line to model the distribution of shoreline points across the time span of 1990–2022. In this study, regression coefficient (R^2) is 0.5986, $p < 0.05$ (Fig. 4d, Table S7).The R-squared values show a good correlation between the dependent and independent variables. Therefore, shoreline change was a significant correlation coefficient.

Chennai (zone 3)

Chennai shore is located on the southeast coast of the Indian peninsula, and also it is one of the major metropolitan coastal cities in the nation. Chennai is the capital of Tamil Nadu state with the longest beach in the country, which is also the second-longest sandy beach in the world called Marina Beach. This zone 3 is considered between the ChPA south to the Adyar River, joining into the Bay of Bengal. Zone 3 is about 9.6 km, with 96 transects used for this shoreline analysis. It has 9101 fishing communities and 12 fish-landing sites, including one significant fish-landing facility. Coovum River estuary (latitude 13° 4′ 2″ N and longitude 80° 17′ 21″ E) on the north of this zone 3 had a 200-m-wide opening into the sea during the monsoon periods between the 1990 and 2000 period. Adyar River estuary (latitude 13° 0′ 50″ N and longitude 80° 16′ 38″ E) on the south of this zone 3 had a

400-m-wide opening into the sea between 1990 and 2000. Satellite image analysis shows that this zone was dominated by accretion (Fig. 5a). This may not only be by the two rivers' sediment supply into the sea but may also be by anthropogenic developmental activities, like ChPA. The findings show the maximum shoreline accretion rate was about 4.21 m/y (EPR) and 6.32 m/y (LRR). The maximum erosion rate was − 1.16 m/y (EPR), and − 0.84 m/y (LRR) was found. At Chennai, shoreline accretion was detected at an average rate of 1.66 m/y (EPR) and 1.78 m/y (LRR) (Fig. 5b, Table S8). In the starting period of 1990, the mean baseline was 667.8 m. The mean baseline was 673.0 m in 1995, 667.6 m in 2000, 701.3 m in 2005, 696.5 m in 2010, 698.7 m in 2015, and 723.4 m in 2020. In 2022, the shoreline accreted, and the present shoreline is located at a distance of 721.3 m from the baseline (Fig. 5c, Table S9). The coastline change analysis is consistent with the results obtained by Mary et al. (2022) who used LRR and EPR to detect shoreline changes in the same location from 2000 to 2019. According to this researcher, the building of the training wall at the Coovum River mouth caused the Chennai shoreline to accrete to a maximum length of roughly 10.5 m. We calculated an LRR of change by using a least-square regression line to model the distribution of shoreline points across the time span of 1990–2022. In this study, regression coefficient (R^2) is 0.8668, $p < 0.0008$ (Fig. 5d, Table S10). The R-squared values show a good correlation between the dependent and independent variables. Therefore, shoreline change was a significant correlation coefficient. The satellite images show evidence of physical changes in the river mouth openings (joining into the sea) and the closing of the river contact into the sea by the accretion. The orientation direction of the river joining also conveys the sediment supply/exchange between the river water and seawater.
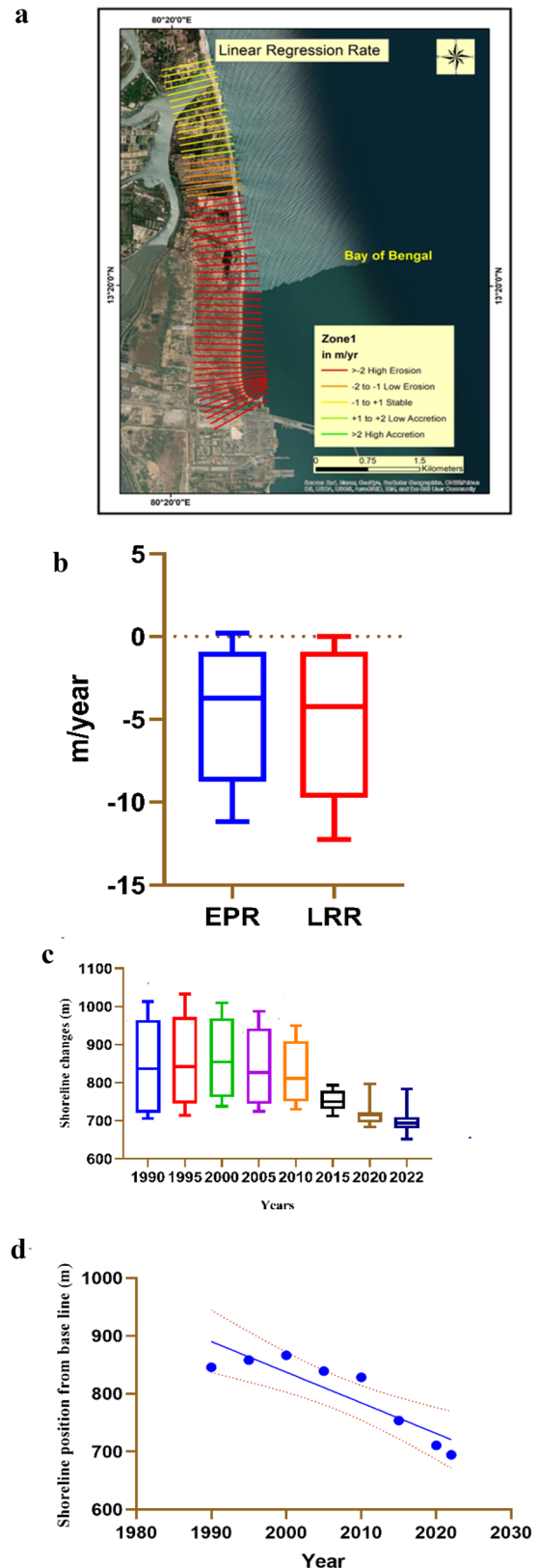
Fig. 4 a Estimations of different shoreline changes (erosion or ▶ accretion) detected at Ennore (zone 2) in Tamil Nadu, India, between 1990 and 2022; **b** box plot of different degrees of erosion and accretion at the Ennore (zone 2) in Tamil Nadu, India, between 1990 and 2022 from LRR, EPR; **c** box plot of change from baseline in Ennore (zone 2) in Tamil Nadu, India, between 1990 and 2022; **d** linear regression rate of shoreline changes. Blue dot represents data points, blue line represents line of regression, and red dashed lines represent the confidence interval

Kovalam (zone 4)

Kovalam is a fishing village located about 30 km south of Chennai City and lies within the districts of Chennai and Chengalpattu. Zone 4 covers about 23.6 km long, with 236 transects between the Adyar River south and Mutukkadu backwater joining the Bay of Bengal. This coastal stretch the major anthropogenic activities, not only within the Chennai City limit beaches, namely, Elliot's Beach/Besant Nagar Beach, Thiruvanmiyur Beach, Palavakkam Beach, and also many more public/private beach resorts, family theme parks like VGP, MGM, etc. along with the fishing communities in the continuous sandy beach up to the mid of the Mutukkadu backwater opening into the Bay of Bengal. Mutukkadu backwater joins with the Bay of Bengal at latitude 12°48′16″ N and longitude 80°14′56″ E. But, the mouth of this backwater close and led to the disconnection with the Bay of Bengal during the non-monsoon period because of the formation of sandy beaches. The satellite images of 1990, 1995, 2000, 2005, 2010, and 2015 show this zone 4 was devoid of hard coastal engineering structures. But, the recent satellite images of 2020 and 2022 show evidence of seawall (latitude 12°48′58″ N and longitude 80°14′5″ E), groins (latitude 12°48′29″ N and longitude 80°14′52″ E), and training wall (latitude 12°48′20″ N and longitude 80°14′56″ E) on the north of the Mutukkadu backwater joining into the sea. This region was not undergoing significant accretion or erosion (Fig. 6a). Based on the findings, the highest shoreline accretion rate was around 2.88 m/y (EPR) and 2.91 m/y (LRR). The study also determined that the maximum erosion rates were − 1.14 m/y (EPR) and − 0.51 m/y (LRR), respectively. The average accretion rate along the Kovalam coast was determined to be 0.91 m/y (EPR) and 0.65 m/y (LRR) (Fig. 6b, Table S11). The study of the shoreline change agrees with the findings
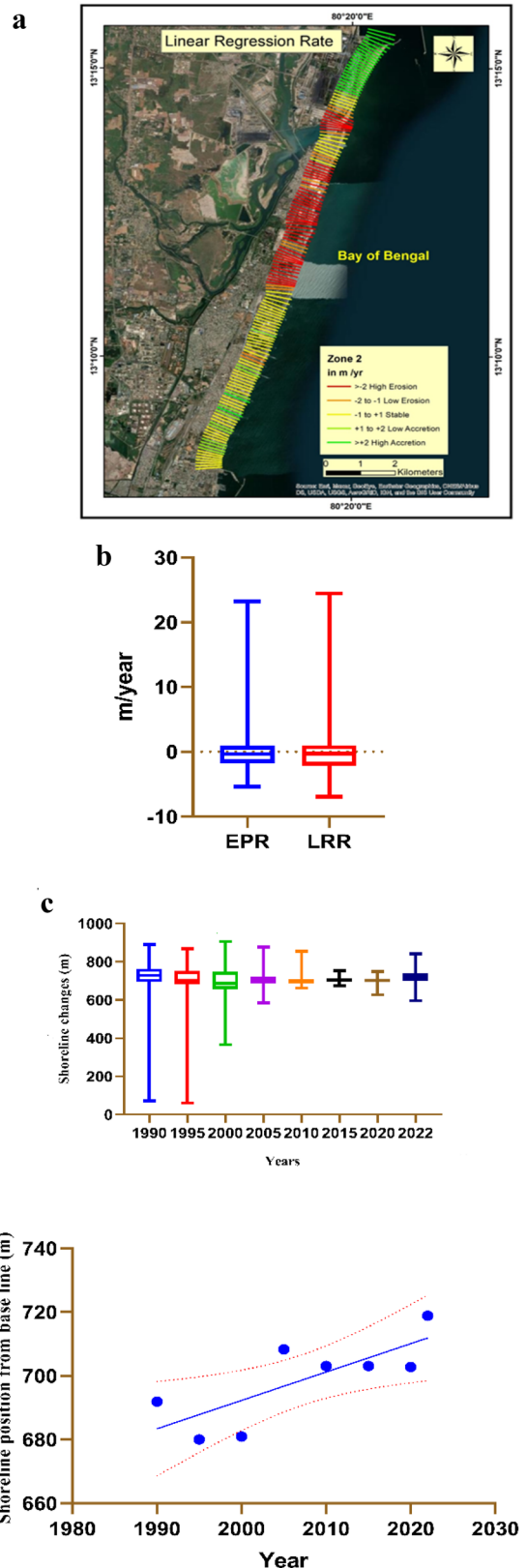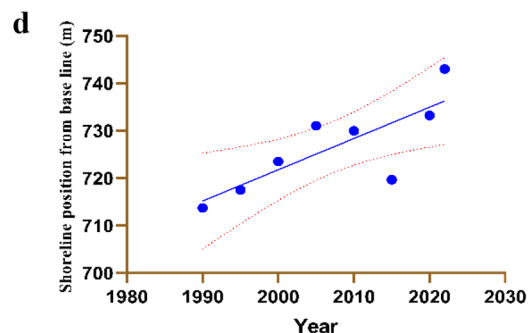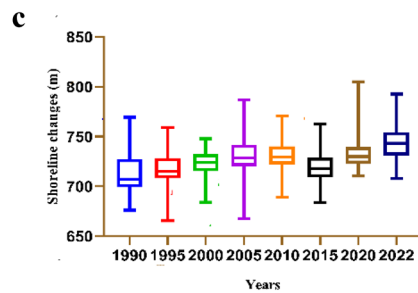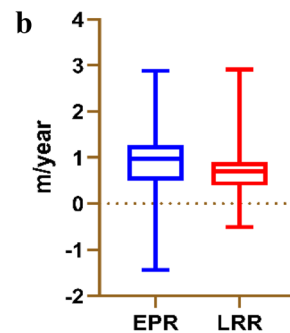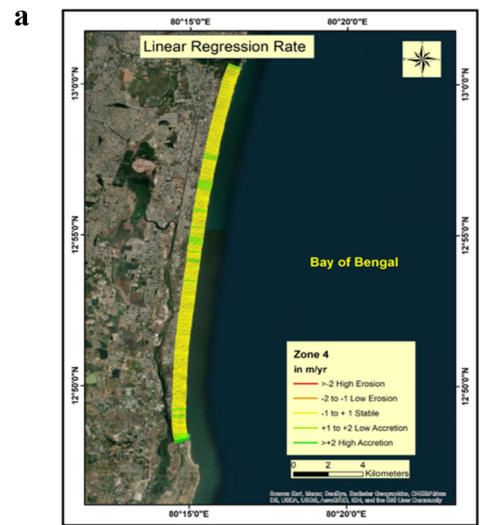
Fig. 5 **a** Estimations of different shoreline changes (erosion or ▶ accretion) detected at Chennai (zone 3) in Tamil Nadu, India, between 1990 and 2022; **b** box plot of different degrees of erosion and accretion at the Chennai (zone 3) in Tamil Nadu, India, between 1990 and 2022 from LRR, EPR; **c** box plot of change from baseline in Chennai (zone 3) in Tamil Nadu, India, between 1990 and 2022, **d** linear regression rate of shoreline changes. Blue dot represents data points, blue line represents line of regression, and red dashed lines represent the confidence interval

of Ayyappan and Thiruvenkatasamy (2018) for the same place in the years 2017 and 2018. Since the groins provide a barrier for transporting and depositing marine sediments, this researcher concludes that the Kovalam shoreline has accreted as a consequence. In 1990, the average baseline was 713.7 m. The mean baseline was 717.5 m in 1995, 723.5 m in 2000, 731.1 m in 2005, 730.0 m in 2010, 719.7 m in 2015, and 733.2 m in 2020 (Fig. 6c, Table S12). Shoreline accretion in 2022 and the existing shoreline's position is 743.0 m from the baseline. The least-square regression line was used to calculate the average annual rate of change along the coast from 1990 to 2022. The R^2 value for this analysis is 0.6366, $p < 0.01$. (Fig. 6d, Table S13). The R-squared values show a good correlation between the dependent and independent variables. Therefore, the shoreline shift had a statistically significant association coefficient.

Mahabalipuram (zone 5)

The Mahabalipuram is 55 km south of Chennai City in the Chengalpattu district. This zone 5 extends between the southern training wall of Mutukkadu backwater to the Mahabalipuram shore temple, about 21.5 km long with 215 transects. This zone has a typical sandy beach with scattered rocky outcrops along the Kovalam and Mahabalipuram coasts. Moreover, this coast has a significant coastal erosion protection structure of groins along the Nemmeli desalination plant and the Tiger Caves. This archaeological site was excavated by the 2004 Indian Ocean Tsunami (IOT). For the most part, the seashore at Mahabalipuram runs northeast to the south west and south of Mahabalipuram. About 5 km west of Mahabalipuram are the backwaters known as the Buckingham canal, which has outlets/openings into the Bay of Bengal in the Kovalam on the north and Kalpakkam in the south. This zone was
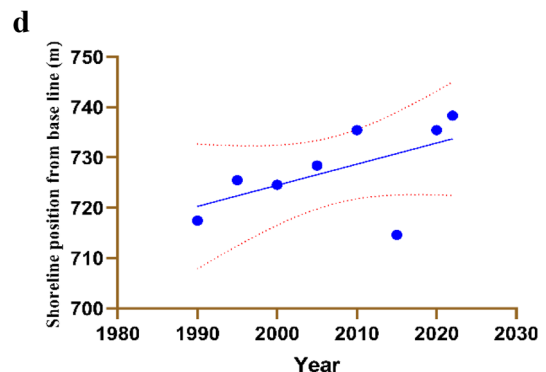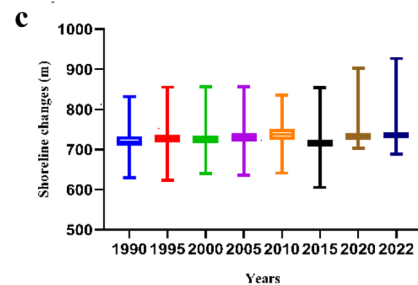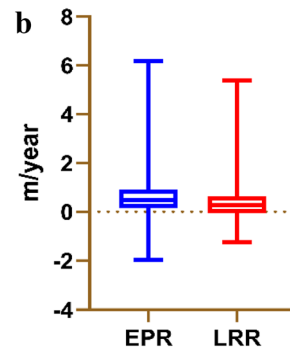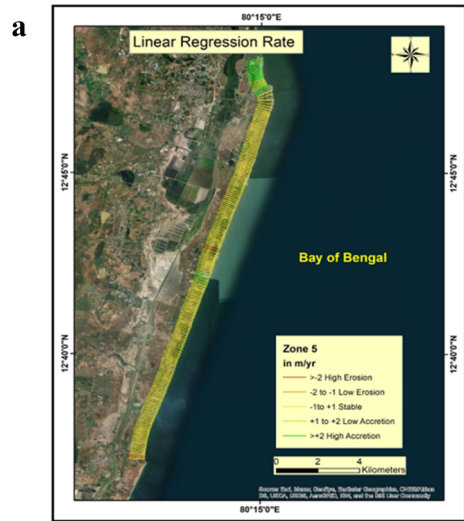
Fig. 6 a Estimations of different shoreline changes (erosion ▶ or accretion) detected at Kovalam (zone 4) in Tamil Nadu, India, between 1990 and 2022; **b** box plot of different degrees of erosion and accretion at the Kovalam (zone 4) in Tamil Nadu, India, between 1990 and 2022 from LRR, EPR; **c** box plot of change from baseline in Kovalam (zone 4) in Tamil Nadu, India, between 1990 and 2022, **d** linear regression rate of shoreline changes. Blue dot represents data points, blue line represents line of regression, and red dashed lines represent the confidence interval

not undergoing significant accretion or erosion (Fig. 7a). This may be due to the absence of continuous non-major anthropogenic activities, industries, fishing harbours, ports, etc. The findings showed a maximum shoreline accretion rate of about 6.18 m/y (EPR) and 5.39 m/y (LRR). The maximum erosion rate was -1.97 m/y (EPR) and -1.24 m/y (LRR). Shoreline accretion was measured at an average rate of 0.65 m/y (EPR) and 0.63 m/y (LRR) at Mahabalipuram (LRR) (Fig. 7b, Table S14). Mariappan and Devi's (2012) findings from the same area and time period (2005–present) are consistent with the results of the shoreline change analysis. Mahabalipuram is secured by a seawall that distends somewhat into the sea (Deepthi, 2012). The impacts of accretion and erosion in these regions may be reduced by a seawall (Natesan et al., 2015). At the start of 1990, the average baseline length was 717.4 m. The mean baseline was 725.5 m in 1995, 724.6 m in 2000, 728.4 m in 2005, 735.4 m in 2010, 714.6 m in 2015, and 735.2 m in 2020. Currently, the coastline is 738.3 m from the baseline, but it is expected to accrete through 2022 (Fig. 7c, Table S15). The least-square regression line calculated the rate of change along the coast from 1990 to 2022. The R-squared value in this analysis is 0.3203 (p-value > 0.05) (Fig. 7d, Table S16). Consequently, the correlation coefficient between shoreline shifts was not statistically significant.
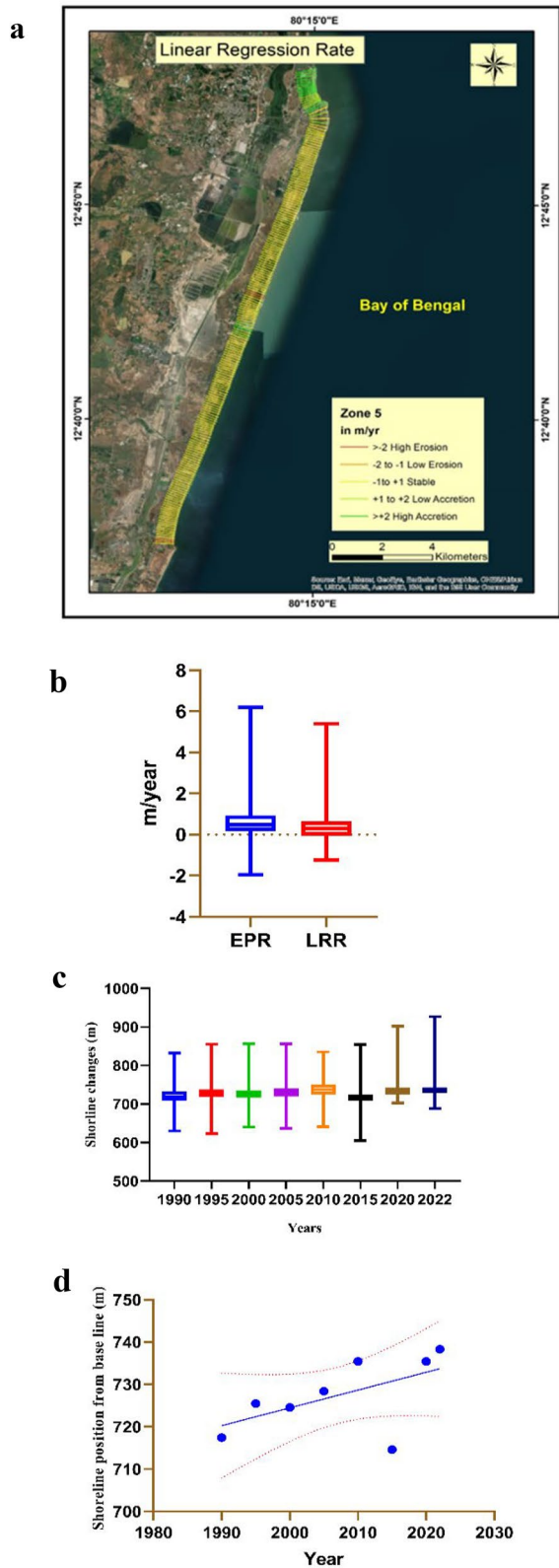
Kalpakkam (zone 6)

The Kalpakkam is located around 60 km south of Chennai in the Chengalpattu district. This zone 6 extends from the north of Mahabalipuram shore temple to the south of Palar river, joining into the Bay of Bengal about 19.4 km with 194 transects. Kalpakkam is home to a number of fishing communities as well as a coastal township connected to the Madras Atomic
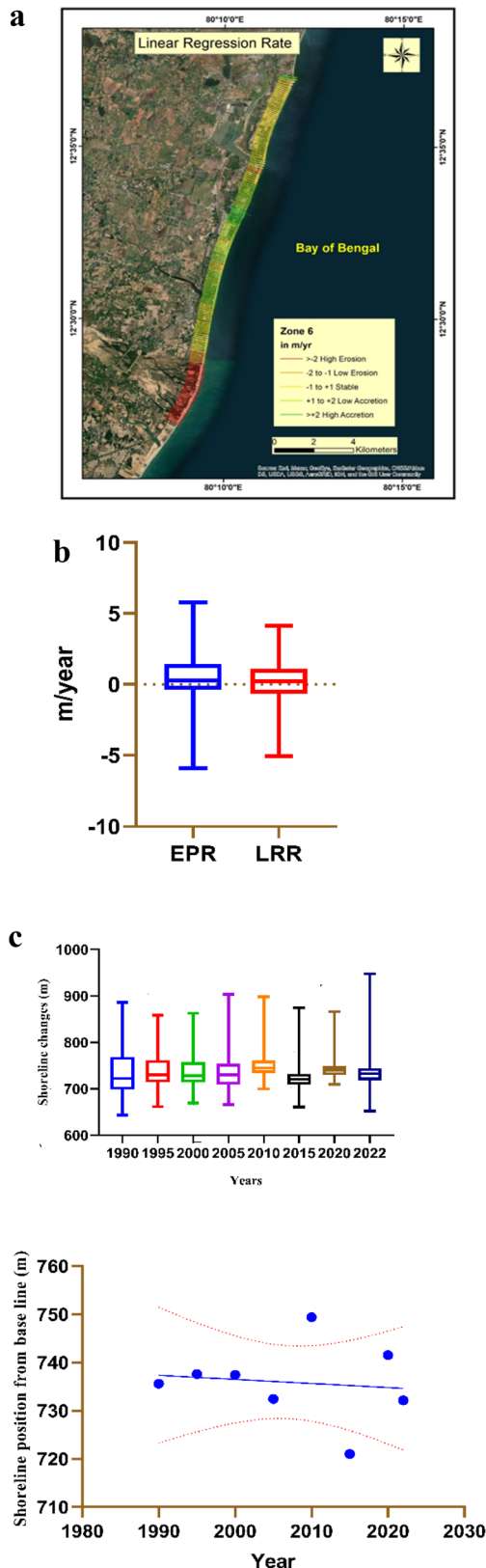
Fig. 7 a Estimations of different shoreline changes (erosion or ▶ accretion) detected at Mahabalipuram (zone 5) in Tamil Nadu, India, between 1990 and 2022; **b** box plot of different degrees of erosion and accretion at the Mahabalipuram (zone 5) in Tamil Nadu, India, between 1990 and 2022 from LRR, EPR; **c** box plot of change from baseline in Mahabalipuram (zone 5) in Tamil Nadu, India, between 1990 and 2022; **d** linear regression rate of shoreline changes. Blue dot represents data points, blue line represents line of regression, and red dashed lines represent the confidence interval

Power Station. The Kalpakkam coastline runs in a straight line from NNE–SSW direction. Major anthropogenic activities were at the shore temple (remnants of the historical Pallava dynasty) at Mahabalipuram and the atomic nuclear power plant of Kalpakkam. There is an inlet opening at (latitude 12°34′35″ N and longitude 80°11′5″ E) the Kalpakkam and also the Palar River join at (latitude 12°27′55″ N and longitude 80° 9′10″ E) the Bay of Bengal. This region's erosion, stability, and accretion rates are all about the same (Fig. 8a). This coastal stretch also witnesses non-major continuous anthropogenic activity and also absence of fishing harbours, ports, etc. According to the findings, the highest rates of shoreline accretion were around 5.78 m/y (EPR) and 4.12 m/y (LRR). Maximum erosion rates were calculated to be -5.99 m/y (EPR) and -5.06 m/y (LRR). The average erosion rates of the Kalpakkam coastline were observed at -0.11 m/y (EPR) and -0.09 m/y (LRR) (Fig. 8b, Table S17). Due to wave-induced longshore currents and the dynamic coastal process, coastal areas experience erosion and accretion at varying rates along their seabeds (Cherian et al., 2012; Hegde, 2010). Low frictional energy loss during wave propagation over a narrow shelf leads to increased coastal erosion because the wave disperses energy along the coast (Vinayaraj et al., 2011). In terms of influencing the relative rates of erosion and accretion along the coast, sediment movement along offshore is a crucial process (Saravanan et al., 2011). The accretionary nature of the coastline and beach-building activities in front of the seawall assures protection from wave impacts without seriously affecting the coastal ecosystem (Deepthi, 2012). The mean baseline was 737.6 m in 1995, 737.4 m in 2000, 732.5 m in 2005, 749.4 m in 2010, 721.0 m in 2015, and 741.5 m in 2020. The current coastline is 732.1 m away from the baseline due to coastal erosion in 2022 (Fig. 8c, Table S18). All coastline points from 1990 to 2022 were fitted with a

a

b

c

d

◄ **Fig. 8 a** Estimations of different shoreline changes (erosion or accretion) detected at Kalpakkam (zone 6) in Tamil Nadu, India, between 1990 and 2022; **b** box plot of different degrees of erosion and accretion at the Kalpakkam (zone 6) in Tamil Nadu, India, between 1990 and 2022 from LRR, EPR; **c** box plot of change from baseline in Kalpakkam (zone 6) in Tamil Nadu, India, between 1990 and 2022; **d** linear regression rate of shoreline changes. Blue dot represents data points, blue line represents line of regression, and red dashed lines represent the confidence interval

least-square regression line to generate an LRR. With a value of 0.01469 ($p > 0.05$), the study's R^2 regression coefficient is statistically insignificant (Fig. 8d, Table S19). Therefore, there is no statistically significant relationship between shoreline changes.

Conclusion

The DSAS tool was used to identify shoreline changes for the 32 years between 1990 and 2022 along the northern Tamil Nadu coasts of India using the USGS Landsat satellite images of 1990, 1995, 2000, 2005, 2010, 2015, 2020, and 2022. The shoreline was extracted using the ISODATA classification system. Based on the USGS Landsat satellite images and the extracted shorelines, DSAS tool was used to generate 1054 transects, out of which 951 transects were used to track changes in the shoreline positions by LRR and EPR methods. The results displayed that the maximum accretion rate was 23.24 m/year (EPR) and 24.46 m/year (LRR), and the maximum erosion rate was -11.15 m/year (EPR) and -12.24 (LRR) observed at the northern coast of Tamil Nadu, India. The results identified two regions with higher rates, namely Kattupalli -11.15 m/year (EPR) and -12.24 (LRR) and Ennore -5.41 (EPR) and -7.00 (LRR). These two coasts had been heavily populated, industrialized, and impacted by man-made buildings while also being subject to erosion. One of the key causes for the influence changes in a coastal environment might be the development of artificial structures (ports, jetties, groins, seawalls, etc.) and the presence of a large population. In addition to the continuous natural wind, waves, swells, tides, currents, coastal flooding, sea level rise, bathymetry, etc., the increased anthropogenic activities (tourists, fishing, etc.) amplify the shoreline changes along with the increased disaster (cyclone) frequency within a year.

Shoreline analysis using satellite remote sensing, GIS, and in situ data will provide the required information for basic to advanced scientific research. The freely available digital satellite images of an area for different long (seasonal, yearly, biannual, decades, etc.) periods can be used to identify the frequently changing location using the appropriate remote sensing and GIS techniques.

Author contribution   T. German Amali Jacintha conceptualized and designed the research. T. German Amali Jacintha and T.Y. Suman analysed the data. T. German Amali Jacintha, Radhika Rajasree, J. Sriganesh, and T.Y. Suman drafted the initial report, which was subsequently revised and edited by all authors.

Data availability   The datasets generated and/or analysed during the current study are available from the corresponding author on reasonable request. The authors have no relevant financial or non-financial interests to disclose.

Declarations

Ethics approval   All authors have read, understood, and have complied as applicable with the statement on "Ethical Responsibilities of Authors" as found in the Instructions for Authors and are aware that with minor exceptions, no changes can be made to authorship once the paper is submitted.

Consent for publication   The manuscript is approved by all authors for publication.

Competing interests   The authors declare no competing interests.

References

Anand, K. V., Sundar, V., Sannasiraj, S. A., Murali, K., Rangarao, V., & Subramanian, B. R. (2011). Littoral transport estimate from the field measurement along north Chennai coast of Tamil Nadu, India. *Asian and Pacific Coasts, 2011*, 1541–1548. https://doi.org/10.1142/9789814366489_0185

Ayyappan, K., & Thiruvenkatasamy, K. (2018). On the hydrodynamics of shoreline morphological changes and its impact on tidal stability in the presence of groins using field measurements at Muttukadu Estuary. *International Journal of Civil Engineering and Technology, 9*, 912–922.

Bagli, S., & Soille, P. (2003). Morphological automatic extraction of Pan-European coastline from Landsat ETM+ images. *Proceedings of the Fifth International Symposium on GIS and Computer Cartography for Coastal Zone Management, Genova, 26 September 2003*, 58–69.

Berberoglu, S., & Akin, A. (2009). Assessing different remote sensing techniques to detect land use/cover changes in the eastern Mediterranean. *International Journal of Applied Earth Observation and Geoinformation, 11*(1), 46–53. https://doi.org/10.1016/j.jag.2008.06.002

Chand, P., & Acharya, P. (2010). Shoreline change and sea level rise along coast of Bhitarkanika wildlife sanctuary, Orissa: An analytical approach of remote sensing and statistical techniques. *International Journal of Geomatics and Geosciences, 1*(3), 436–455.

Chen, C., Bu, J., Zhang, Y., Zhuang, Y., Chu, Y., Hu, J., & Guo, B. (2019). The application of the tasseled cap transformation and feature knowledge for the extraction of coastline information from remote sensing images. *Advances in Space Research, 64*, 1780–1791. https://doi.org/10.1016/j.asr.2019.07.032

Cherian, A., Chandrasekar, N., Gujar, A. R., & Rajamanickam, G. V. (2012). Coastal erosion assessment along the southern Tamil Nadu coast, India. *International Journal of Earth Sciences & Engineering, 5*(02), 352–357.

Crowell, M., Douglas, B. C., & Leatherman, S. P. (1997). On forecasting future U.S. shoreline positions: a test of algorithms. *Journal of Coastal Research, 13*(4), 1245–1255.

Deepika, B., Avinash, K., & Jayappa, K. S. (2014). Shoreline change rate estimation and its forecast: Remote sensing, geographical information system and statistics-based approach. *International Journal of Environmental Science and Technology, 11*, 395–416. https://doi.org/10.1007/s13762-013-0196-1

Deepthi, K. (2012). Unraveling the shelf sediment dynamics using field data, remote sensing and numerical model for Kalpakkam, southeast coast of India. *(Doctor of Philosophy, Dissertation, Anna University, Chennai)*.

Dolan, R., Fenster, M. S., & Holme, S. J. (1991). Temporal analysis of shoreline recession and accretion. *Journal of Coastal Research, 7*(3), 723–744.

Douglas, B. C., & Crowell, M. (2000). Long-term shoreline position prediction and error propagation. *Journal of Coastal Research, 16*(1), 145–152.

Genz, A. S., Fletcher, C. H., Dunn, R. A., Frazer, L. N., & Rooney, J. J. (2007). The predictive accuracy of shoreline change rate methods and alongshore beach variation on Maui. *Hawaii. Journal of Coastal Research, 23*(1), 87–105.

Hegde, A. V. (2010). Coastal erosion and mitigation methods–Global state of art. *Indian Journal of Geo-Marine Sciences, 39*(4), 521–530.

Himmelstoss, E. A., Henderson, R. E., Kratzmann, M. G., & Farris, A. S. (2021). Digital Shoreline Analysis System (DSAS) version 5.1 user guide: U.S. Geological Survey Open-File Report, 2021–1091. https://doi.org/10.3133/ofr20211091

Jayakumar, K., & Malarvannan, S. (2016). Assessment of shoreline changes over the northern Tamil Nadu coast, South India using WebGIS techniques. *Journal of Coastal Conservation, 20*(6), 477–487.

Kaliraj, S., Chandrasekar, N., & Magesh, N. S. (2015). Evaluation of coastal erosion and accretion processes along the southwest coast of Kanyakumari, Tamil Nadu using geospatial techniques. *Arabian Journal of Geosciences, 8*(1), 239–253. https://doi.org/10.1007/s12517-013-1216-7

Kankara, R. S., Mohan, R., & Venkatachalapathy, R. (2013). Hydrodynamic modelling of Chennai coast from a coastal zone management perspective. *Journal of Coastal Research, 29*(2), 347–357.

Kannan, R., Anand, K. V., Sundar, V., Sannasiraj, S. A., & Rangarao, V. (2014). Shoreline changes along the Northern coast of Chennai port, from field measurements. *ISH Journal of Hydraulic Engineering, 20*(1), 24–31. https://doi.org/10.1080/09715010.2013.821789

Kumaravel, S., Ramkumar, T., Gurunanam, B., Suresh, M., & Dharanirajan, K. (2013). An application of remote sensing and GIS based shoreline change studies–A case study in the Cuddalore District, East Coast of Tamil Nadu, South India. *International Journal of Innovative Technology and Exploring Engineering, 2*(4), 211–215.

Li, D., & Tang, P. (2013). A sensor specified method based on spectral transformation for masking cloud in Landsat data. *IEEE Journal of Selected Topics in Applied Earth Observations and Remote Sensing, 6*(3), 1619–1627. https://doi.org/10.1109/JSTARS.2013.2259469

Li, R., Di, K., & Ma, R. (2001). A comparative study of shoreline mapping techniques. *(The Fourth International Symposium on Computer Mapping and GIS for Coastal Zone Management). Halifax, Nova Scotia, Canada.*

Liu, H., & Jezek, K. C. (2004). Automated extraction of coastline from satellite imagery by integrating Canny edge detection and locally adaptive thresholding methods. *International Journal of Remote Sensing, 25*(5), 937–958. https://doi.org/10.1080/0143116031000139890

Maiti, S., & Bhattacharya, A. K. (2009). Shoreline change analysis and its application to prediction: A remote sensing and statistics-based approach. *Marine Geology, 257*(1–4), 11–23. https://doi.org/10.1016/j.margeo.2008.10.006

Marfai, M. A., Almohammad, H., Dey, S., Susanto, B., & King, L. (2008). Coastal dynamic and shoreline mapping: Multi-sources spatial data analysis in Semarang Indonesia. *Environmental Monitoring and Assessment, 142*(1), 297–308. https://doi.org/10.1007/s10661-007-9929-2

Mariappan, V. E., & Devi, R. S. (2012). Chennai coast vulnerability assessment using optical satellite data and GIS techniques. *International Journal of Remote Sensing & GIS, 1*(3), 175–182.

Mary, G. M. R., Sundar, V., & Sannasiraj, S. A. (2022). Analysis of shoreline change between inlets along the coast of Chennai, India. *Marine Georesources & Geotechnology, 40*(1), 26–35. https://doi.org/10.1080/1064119X.2020.1856241

Mills, J. P., Buckley, S. J., Mitchell, H. L., Clarke, P. J., & Edwards, S. J. (2005). A geomatics data integration technique for coastal change monitoring. *Earth Surface Processes and Landforms, 30*(6), 651–664. https://doi.org/10.1002/esp.1165

Mujabar, P. S., & Chandrasekar, N. (2013). Shoreline change analysis along the coast between Kanyakumari and Tuticorin of India using remote sensing and GIS. *Arabian Journal of Geosciences, 6*(3), 647–664. https://doi.org/10.1007/s12517-011-0394-4

Nassar, K., Mahmod, W. E., Masria, A., Fath, H., & Nadaoka, K. (2018). Numerical simulation of shoreline responses in the vicinity of the western artificial inlet of the Bardawil Lagoon, Sinai Peninsula, Egypt. *Applied Ocean Research, 74*, 87–101. https://doi.org/10.1016/j.apor.2018.02.015

Natesan, U., Parthasarathy, A., Vishnunath, R., Kumar, G. E. J., & Ferrer, V. A. (2015). Monitoring longterm shoreline changes along Tamil Nadu, India using geospatial techniques. *Aquatic Procedia, 4*, 325–332. https://doi.org/10.1016/j.aqpro.2015.02.044

Pandian, P. K., Ramesh, S., Murthy, M. V. R., Ramachandran, S., & Thayumanavan, S. (2004). Shoreline changes and near shore processes along Ennore coast, east coast of South India. *Journal of Coastal Research, 20*(3), 828–845.

Raj, N., Gurugnanam, B., Sudhakar, V., & Francis, P. G. (2019). Estuarine shoreline change analysis along The Ennore river mouth, south east coast of India, using digital shoreline analysis system. *Geodesy & Geodynamics, 10*, 205–212. https://doi.org/10.1016/j.geog.2019.04.002

Raj, N., Rejin Nishkalank, R. A., & Chrisben Sam, S. (2020). Coastal shoreline changes in Chennai: Environment impacts and control strategies of southeast coast Tamil Nadu. Hussain, C. (eds) *Handbook of Environmental Materials Management*, 1–14. Cham: Springer. https://doi.org/10.1007/978-3-319-58538-3_223-1

Rasuly, A., Naghdifar, R., & Rasoli, M. (2010). Monitoring of Caspian Sea coastline changes using object-oriented techniques. *Procedia Environmental Sciences, 2*, 416–426. https://doi.org/10.1016/j.proenv.2010.10.046

Roy, S., Mahapatra, M., & Chakraborty, A. (2018). Shoreline change detection along the coast of Odisha, India using digital shoreline analysis system. *Spatial Information Research, 26*, 563–571. https://doi.org/10.1007/s41324-018-0199-6

Saranathan, E., Chandrasekaran, R., Soosai Manickaraj, D., & Kannan, M. (2011). Shoreline changes in Tharangampadi Village, Nagapattinam District, Tamil Nadu, India-A case study. *Journal of the Indian Society of Remote Sensing, 39*, 107–115. https://doi.org/10.1007/s12524-010-0052-4

Saravanan, S., Chandrasekar, N., Mujabar, P. S., & Hentry, C. (2011). An overview of beach morphodynamic classification along the beaches between Ovari and Kanyakumari, Southern Tamil Nadu coast, India. *Physical Oceanography, 21*, 129–141. https://doi.org/10.1007/s11110-011-9110-x

Sherman, D. J., & Bauer, B. O. (1993). Coastal geomorphology through the looking glass. *Geomorphology, 7*(1–3), 225–249. https://doi.org/10.1016/0169-555X(93)90018-W

Sriganesh, J., Saravanan, P., & Ram Mohan, V. (2015). Remote sensing and GIS analysis on Cuddalore Coast of Tamil Nadu, India. *Journal of Advanced Research in Geo Sciences & Remote Sensing, 2*(3&4), 94–108.

Thieler, E. R., Himmelstoss, E. A., Zichichi, J. L., & Ergul, A. (2017). Digital Shoreline Analysis System (DSAS) version 4.0—An ArcGIS extension for calculating shoreline change (ver. 4.4, July 2017): U.S. Geological Survey Open-File Report 2008–1278. https://doi.org/10.3133/ofr20081278

Van, T. T., & Binh, T. T. (2009). Application of remote sensing for shoreline change detection in Cuu Long estuary. *Environmental Science, Mathematics.*

Vinayaraj, P., Johnson, G., Udhaba Dora, G., Sajiv Philip, C., Sanil Kumar, V., & Gowthaman, R. (2011). Quantitative estimation of coastal changes along selected locations of Karnataka, India: A GIS and remote sensing approach. *International Journal of Geosciences, 2*(4), 385–393. https://doi.org/10.4236/ijg.2011.24041